A NEW MILKY WAY HALO STAR CLUSTER IN THE SOUTHERN GALACTIC SKY

E. Balbinot[1,2], B. X. Santiago[1,2], L. da Costa[2,3], M. A. G. Maia[2,3], S. R. Majewski[4], D. Nidever[5], H. J. Rocha-Pinto[2,6], D. Thomas[7], R.H. Wechsler[8], B. Yanny[9]

Draft version November 1, 2018

ABSTRACT

We report on the discovery of a new Milky Way companion stellar system located at $(\alpha_{J2000}, \delta_{J2000}) = (22^h10^m43.15^s, 14°56'58.8'')$. The discovery was made using the eighth data release of SDSS after applying an automated method to search for overdensities in the Baryon Oscillation Spectroscopic Survey footprint. Follow-up observations were performed using CFHT/MegaCam, which reveal that this system is comprised of an old stellar population, located at a distance of $31.9^{+1.0}_{-1.6}$ kpc, with a half-light radius of $r_h = 7.24^{+1.94}_{-1.29}$ pc and a concentration parameter of $c = \log_{10}(r_t/r_c) = 1.55$. A systematic isochrone fit to its color-magnitude diagram resulted in $\log(age/yr) = 10.07^{+0.05}_{-0.03}$ and $[Fe/H] = -1.58^{+0.08}_{-0.13}$. These quantities are typical of globular clusters in the MW halo. The newly found object is of low stellar mass, whose observed excess relative to the background is caused by 95 ± 6 stars. The direct integration of its background decontaminated luminosity function leads to an absolute magnitude of $M_V = -1.21 \pm 0.66$. The resulting surface brightness is $\mu_V = 25.90$ mag/arcsec^2. Its position in the M_V vs. r_h diagram lies close to AM4 and Koposov 1, which are identified as star clusters. The object is most likely a very faint star cluster — one of the faintest and lowest mass systems yet identified.

Subject headings: globular clusters: general — galaxies: dwarf — Local Group

1. INTRODUCTION

Recent large surveys such as Sloan Digital Sky Survey (SDSS) and the 2-Micron All Sky Survey (2MASS) have delivered an enormous amount of data about the stellar populations of the Milky Way (MW). These studies have probed a new regime in parameter space of Milky Way satellites, by significantly expanding the volume over which the faintest systems can be detected, and have revealed a wealth of new objects. One striking discovery from these surveys is the myriad of substructures that populate the MW structural components, including stellar streams from disrupting satellite galaxies and tidal tails from globular clusters (e.g Rockosi et al. 2002; Majewski et al. 2003; Rocha-Pinto et al. 2004; Newberg et al. 2010). It has included the exciting discovery of a new class of faint dwarf galaxies (e.g. Willman et al. 2005; Belokurov et al. 2006; Irwin et al. 2007; Walsh et al. 2009), which may elucidate our understanding of small-scale structure in the dark matter distribution and of galaxy formation at the lowest masses. In addition, a handful of very faint stellar systems have been identified in the outer halo (Koposov et al. 2007; Belokurov et al. 2010; Muñoz et al. 2012; Fadely et al. 2011), with somewhat different properties from more massive clusters.

Studies of extragalactic star cluster systems have also revealed the existence of diffuse and low surface brightness stellar systems around luminous galaxies, such as Faint Fuzzies (FF) and Diffuse Star Clusters (DSC) (Larsen & Brodie 2000; Peng et al. 2006). Studying nearby counterparts of these elusive objects will allow us to better constrain their structure, dynamics, and formation histories.

A significant population of MW satellites is very likely still left undiscovered (Tollerud et al. 2008; Willman 2010). Future deep surveys, such as the Dark Energy Survey[10] and the Large Synoptic Survey Telescope [11], will allow very faint systems to be probed much further out in the Galactic Halo, and are likely to provide important new clues to the formation mechanism of globular clusters, to the hierarchical buildup of the Milky Way system, to galaxy formation physics in low masses systems, and to the abundance and properties of the smallest scale structures in the Universe (Rossetto et al. 2011).

In this work we present the discovery of a new stellar system in the MW halo. The object is located at $(\alpha_{J2000}, \delta_{J2000}) = (22^h10^m43.15^s, 14°56'58.8'')$, or $(l, b) = (75.1735°, -32.6432°)$, in the Pegasus constellation. Its standard SDSS object name is SDSS J2211+1457, although in this work we choose to call it by a shorter name, Balbinot 1. This paper is organized

Correspondece to: balbinot@if.ufrgs.br

[1] Instituto de Física, UFRGS, CP 15051, Porto Alegre, RS 91501-970, Brazil
[2] Laboratório Interinstitucional de e-Astronomia - LIneA, Rua Gal. José Cristino 77, Rio de Janeiro, RJ - 20921-400, Brazil
[3] Observatório Nacional, Rua Gal. José Cristino 77, Rio de Janeiro, RJ - 22460-040, Brazil
[4] Department of Astronomy, University of Virginia, Charlottesville, VA 22904-4325, USA
[5] Department of Astronomy, University of Michigan, Ann Arbor, MI 48109-1042, USA
[6] Observatório do Valongo, Universidade Federal do Rio de Janeiro, Rio de Janeiro RJ 20080-090, Brazil
[7] Institute of Cosmology and Gravitation, University of Portsmouth, Portsmouth, Hampshire PO1 2UP, UK
[8] Kavli Institute for Particle Astrophysics and Cosmology; SLAC National Accelerator Laboratory; Department of Physics, Stanford University, Stanford, CA 94305, USA
[9] Fermi National Laboratory, P.O. Box 500, Batavia, IL 60510-5011, USA

[10] http://darkenergysurvey.org
[11] http://www.lsst.org

as follows. In section 2 we describe the data and methods that led to this discovery. In section 3 the follow-up observations and data reduction are briefly explained. In section 4 we quantify the properties of the object in section 5 and discuss the nature of Balbinot 1 in comparison to other satellite systems discovered in the MW. This object is likely a very old stellar cluster, one of the lowest mass and lowest surface brightness objects yet detected.

2. DATA AND METHOD

The Baryon Oscillation Spectroscopic Survey (BOSS) is one of the four surveys that belong to the Sloan Digital Sky Survey III (SDSS-III). Its imaging stage is now complete with photometry in the $ugriz$ system for $\sim 8 \times 10^7$ sources covering a region of ~ 2000 deg^2 in the southern Galactic hemisphere was released in January 2011 as part of the SDSS Data Release 8 (DR8; Aihara et al. 2011). So far, no systematic search for MW faint satellites has been published in the BOSS footprint. Our discovery data were taken from the DR8 `PhotoPrimary` view table. A *clean* sample was defined by selecting those objects flagged as reliable stars or galaxies (see detection process below).

To search for stellar systems in a large area of the sky, we developed an automated tool called `FindSat`. The algorithm closely follows the work of Koposov et al. (2008) and Walsh et al. (2009). There are three main steps in the algorithm. First a color-magnitude cut based on stellar evolutionary models is applied to enhance the presence of old metal-poor stellar populations relative to field stars. Next, `FindSat` uses this filtered stellar sample and creates a density map on the sky plane. Finally, the density map is convolved with a kernel that is the difference between two Gaussians, one with the angular size of a typical Milky Way (MW) satellite ($\sim 4 - 8'$), and the other much wider, used to smooth out any remaining large scale structure on the map.

Source detection is performed on the convolved map using `SExtractor` (Bertin & Arnouts 1996). To circumvent misidentification due to poor star-galaxy separation, we apply identical steps to build density maps of sources classified as galaxies by the SDSS reduction pipeline and apply SExtractor to them. For a given detected source, `FindSat` then compares the signals in the smoothed stellar and galaxy density images as determined by SExtractor, (S_* and S_{gal}, respectively). Known faint satellites tend to fall in the low S_{gal} and high S_* locus of S_{gal} vs. S_* plane. We use this region to select our new satellite candidates. We also compare the position of these new overdensities with those of known objects found in Abell, Globular Clusters, and NGC catalogs, to remove any known object that may share the same locus of the S_{gal} vs. S_* plane.

For the BOSS region we ran `FindSat` using color-magnitude cuts based on four Padova evolutionary models (Girardi et al. 2002) with ages of 8 and 14 Gyr and $Z = [0.001, 0.006]$. We tuned our CMD filter to search search for objects at five distance moduli $(m - M) = [18.0, 19.0, 20.0, 21.0, 22.0]$. Visual inspection of the detected candidates was carried out, revealing Balbinot 1 as a faint overdensity of blue sources consistent with them being stars. However, deeper and higher spatial resolution images were required to investigate the nature of Balbinot 1.
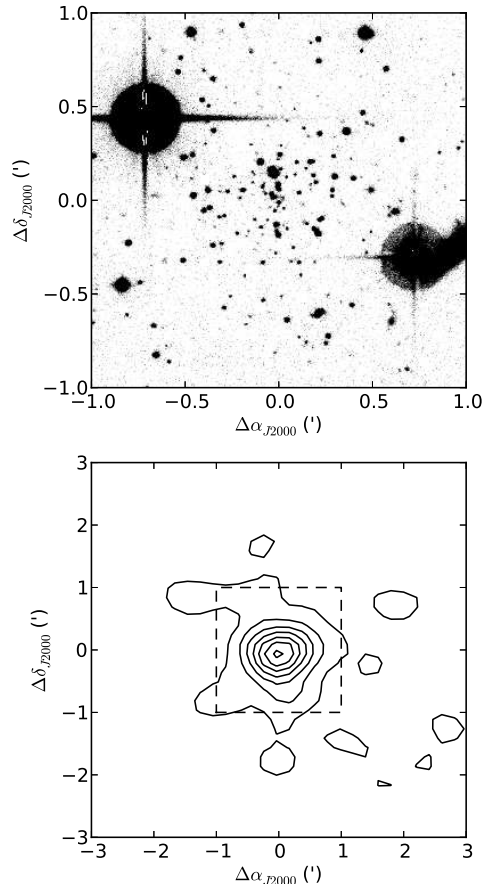
Figure 1. *Bottom panel:* the isodensity contours built using the list of sources detected by Terapix. The contour levels are for $[8, 16, 24, 32, 40]$ stars/$arcmin^2$. The dashed box shows a $1' \times 1'$ region for which we show the combined g band image in the *top panel*.

3. FOLLOW-UP OBSERVATIONS

In the first semester of 2012, we obtained follow-up observations of Balbinot 1 using MegaCam, which is installed in the Canada-France-Hawaii-Telescope (CFHT). MegaCam is a mosaic 36 CCDs, each with $2048 \times 4612 pix$. The total field of view (FOV) is $0.96 \times 0.94 deg$, with a pixel scale of $\sim 0.19\ ''/pix$.

We designed the observations to reach the magnitude of the main sequence turn-off (MSTO) of a 10 Gyr stellar population at 150 kpc distance with $S/N \sim 10$. Exposure times of 2800 s in the g band and 3800 s in the r band were required. The total exposure time was divided into 6 dithering exposures for each passband to avoid scattered light from bright stars, saturation, and also to cover the smaller gaps between the CCDs. The observations were carried out under photometric conditions, seeing was always below $0.8''$, and the airmass below 1.15.

The basic reduction of the images (overscan and bias subtraction, and flatfielding) was done by the CFHT team. The images were geometrically corrected, registered and co-added by Terapix, which uses the Astro-

matic toolkit[12]. Therefore, source detection is based on SExtractor. Point spread function (PSF) photometry was carried out using DAOPHOT (Stetson 1994). The input coordinates list for the stars measured using DAOPHOT was the one provided by Terapix. This list presented less spurious detections than the one from DAOFIND. Photometric calibration was achieved using bright and non-saturated $(19 < g_{SDSS} < 21)$ stars in the observed field, whose instrumental magnitudes were then compared to those from SDSS. We found 536 matches which we used to find a calibration equation composed of a photometric zero point and a color term. The equation coefficients were found by means of a least square fit using sigma clipping rejection. Our mean calibration residuals are of 0.024 in the g band and 0.019 in the r band.

The observed MegaCam field shows little differential reddening. Using the dust maps from Schlegel et al. (1998) we find a value of E(B-V) = 0.060 at position of Balbinot 1 and a standard deviation of 0.0014 across the whole field.

Thus, differential reddening is not likely to contribute significantly to our analysis. Nonetheless we choose to correct for reddening using the value of E(B-V) at the position of each star in the MegaCam field. We adopt $R_V = 3.1$ and the coefficients from Cardelli et al. (1989) to compute the extinction in the CFHT passbands.

Figure 1 shows a stacked g band image centered on Balbinot 1 (top panel). We also show isodensity contours of our detected sources (bottom panel). A clear overdensity of stars is seen on both panels of the figure very close to where the FindSat candidate was originally identified.

4. RESULTS

From Figure 1 it is evident that there is a concentration of stellar-like objects in the observed region. To confirm its stellar nature we must analyze its CMD. In Figure 2 we show the extinction corrected $(g - r) \times g$ CMDs. In the top left panel we show the CMD based on the SDSS discovery data. On the top right panel we show the CMD from our follow up CFHT images. In both cases the stars are restricted to a radius of $150''$ from the visual center of Balbinot 1. To discard Balbinot 1 as a density fluctuation of field stars we also show (*bottom left panel*) the CMD for a ring well away from the object center covering the same area on the sky. By comparing these panels we not only clearly confirm the excess of stars around the position of Balbinot 1 but also conclude that the distribution of these stars on the CMD plane is consistent with a simple stellar population (SSP). An obvious MSTO is seen at $(g - r) \simeq 0.21$ and $g \simeq 21.4$, in connection to an RGB stretching up to $(g - r) \simeq 0.6$ and $g \simeq 18.5$.

The bottom right panel in Figure 2 shows the MSTO region in detail. We also show the best fitting Padova isochrone (Girardi et al. 2002). It corresponds to an age of $11.7^{+1.4}_{-0.8}$ Gyr and an abundance of $Z = 0.0005$, or $[Fe/H] = -1.58^{+0.08}_{-0.13}$ at a distance of $d_\odot = 31.9^{+1.0}_{-1.6}$ kpc. In the same panel we show the effect of varying the distance modulus within its fit uncertainties. The isochrone fit was performed by means of a χ^2 minimization of the
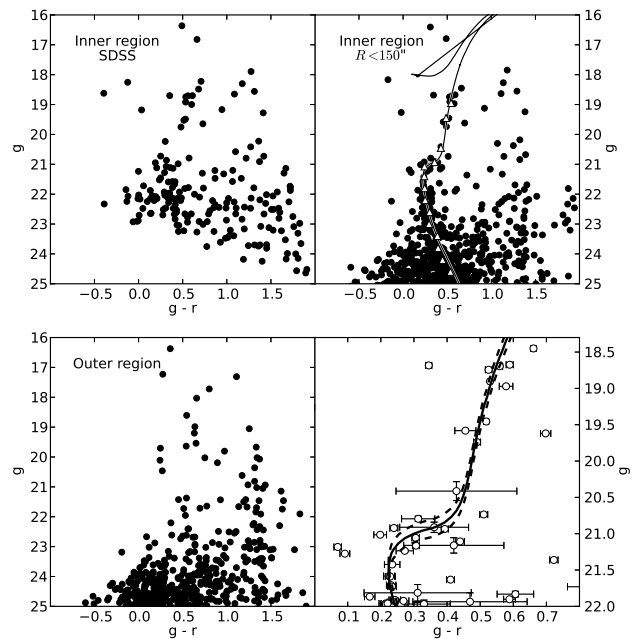
Figure 2. *Top left panel*: $(g - r) \times g$ CMD for SDSS measured sources inside a radius of $150''$ from the visual center of Balbinot 1. *Top right panel*: the CMD for the same region as the previous panel but showing sources from our CFHT photometry. The white triangles show the object ridge line. *Bottom left panel:* CMD for sources located in a ring far away from the object center. The area of the ring is the same as the area of the inner region. In the *bottom right panel* we show zoomed in version of the top right panel around the MSTO region; we also show the photometric errors for each source. The best fit isochrone is shown as a solid line. The isochrones with upper and lower limits of distance modulus are shown by the dashed lines.

CMD distance between the cluster ridge line and the isochrone set. Our model grid goes from 9.8 to 10.12 in $log(age/yr)$ with a step of 0.01, and from 0.0001 to 0.004 in Z, with steps of 0.0001. We adopt a step of 0.01 in distance modulus and a range from 16.0 to 18.0. The best model is the one that minimizes χ^2. The uncertainties are derived from models that have values of $\chi^2 = \chi^2_{min} + 1$.

We stress that the best fit isochrone and its associated parameters are somewhat dependent on the stellar evolution model and on the model grid. In fact, our quoted metallicity uncertainty is comparable to the Padova grid resolution for this parameter. Also, the discrepancies among different evolutionary models are much larger than our quoted uncertainties. For a comprehensive approach to this problem we refer to Kerber & Santiago (2009).

4.1. *Radial profile and half-mass radius*

To quantify the size and concentration of Balbinot 1 we built the radial density profile (RDP) by counting stars in annuli around its center. To increase contrast relative to the background, only stars within 2σ in color away from the best fit isochrone were selected, where σ is the mean photometric error at a given magnitude. The data was also cut at $g < 24$ to avoid photometric
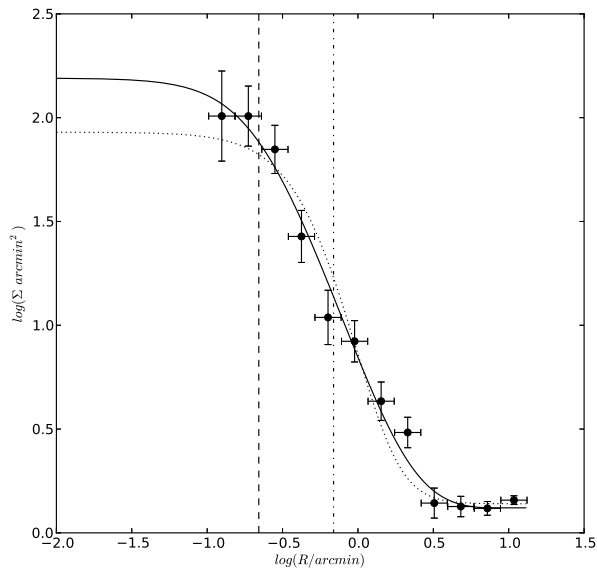
Figure 3. The radial density profile for Balbinot 1 with 1σ error bars in the y direction. The error bars in the x direction are the bin sizes. The solid line shows the best fit King profile. The dashed vertical line shows the position of the core radius. The dot-dashed line shows the half-mass radius, and the dotted line shows the corresponding plummer profile.

incompleteness. The result is shown in Figure 3 where a very peaked distribution of stars is visible.

In order to avoid the binning complications that arise when trying to fit a RDP we chose a Maximum Likelihood (ML) approach. The method we use here follows closely the one described in Martin et al. (2008).

The ML fit was carried out using stars in the range $0.0 \leq R \leq 12'$ and fitted both a King and a Plummer model. This limit was chosen to avoid the large CCD gap of MegaCam. The best fitted models are shown as the solid and dotted lines in Figure 3, respectively. For the King profile we derive $r_{core} = 0.22^{+0.10}_{-0.06}{}'$ and $r_{tidal} = 7.85^{+4.15^*}_{-3.40}{}'$. And the Plummer profile fit yields $r_s = 0.60^{+0.16}_{-0.11}{}'$ and a total number of stars $M^* = 94.7 \pm 5.9$. The uncertainty in each parameter is estimated using the likelihood-ratio approximation, where likelihood values near the maximum approaches a chi-squared distribution. The uncertainties are taken as the 90% confidence level of the chi-square distribution. For the Plummer profile we also kept the center of Balbinot 1 as a free parameter. This allowed us to find the best center and its uncertainty. The best center was then used in the King profile fit. Notice that the upper bound of the tidal radius uncertainty is outside the range of R available in our observations. For simplicity we have adopted the upper bound as the largest radii available, that is $12'$.

For the Plummer profile the half-mass radius is easily obtained from the relation $r_h = 1.305 r_s$, yielding the value of $r_h = 0.78^{+0.21}_{-0.14}{}'$. For the King model we made an estimate of the half-mass radius as follows. We first integrated the profile from zero to the limiting radius and subtracted the expected number of background stars. The result of this operation yields the total num-

ber of observed stars that should belong to Balbinot 1 N_{obs}. We then compute the half-mass radius as the radius which contains $N_{obs}/2$ stars, again taking care to subtract off the expected background sources. We obtain $r_h = 0.69^{+0.33}_{-0.25}{}'$. The two estimates of r_h agree within the uncertainties. Since the Plummer model is widely used in most studies of satellites, we choose to use the half-mass radius estimated from it.

4.2. Total luminosity

The total luminosity of Balbinot 1 is dominated by bright red giant branch (RGB) stars and possibly a few red clump (RC) stars, although Figure 2 does not reveal any obvious RC star in the inner $150''$ region. The small number of evolved stars in the RGB and, most especially, in the RC, indicates that Balbinot 1 is a low mass stellar system, more consistent with being a star cluster than a dwarf galaxy. Given its low stellar mass, to properly estimate the total luminosity of Balbinot 1 one must take into account the background (and foreground) star contamination.

We first built the observed luminosity function (LF) of Balbinot 1 by counting stars as a function of magnitude inside a circle of $150''$ radius from the cluster center and in a ring with inner border at $300''$ and outer at $550''$. We subtracted the area weighted star counts in the ring from the area weighted counts in the inner circle. This results in an observed LF for Balbinot 1 already decontaminated from field stars. The adopted ring is 10 times larger than the cluster circle to minimize fluctuations in the subtracted field contamination. To build the LFs we again applied a magnitude cut of $g < 24.0$ to avoid incompleteness.

The total magnitude is obtained by direct integration of the background decontaminated LF. Using the uncertainty on each bin of the LF and a bootstrap method we derive the uncertainty on the total magnitude. The final value is $M_V = -1.21 \pm 0.66$ for Balbinot 1. Coupling the M_V value with the r_h estimate yields a surface brightness of $\mu_V = 25.90$ mag/arcsec^2. The value of M_V of Balbinot 1 is comparable to the value obtained for Muñoz 1. This luminosity is also comparable to that of SEGUE 3 (Belokurov et al. 2010; Fadely et al. 2011).

5. SUMMARY AND DISCUSSION

In this paper we report on the discovery of a new stellar system in the MW halo, found the SDSS-III/BOSS footprint in the Southern Galactic hemisphere. Its confirmation as a genuine stellar system required deep follow-up imaging from CFHT. By means of a theoretical isochrone fit, we derived a heliocentric distance of $31.9^{+1.0}_{-1.6}$ kpc , an old age of $11.7^{+1.4}_{-0.8}$ Gyr, and a metallicity of [Fe/H] $= -1.58^{+0.08}_{-0.13}$. We also found that a King profile provides a good description of its structure; the best fit profile has a core radius of $r_c = 2.04^{+0.93}_{-0.56}$ pc[1], a limiting radius of $r_t = 72.84^{+38.51}_{-31.55}$ pc, and a projected half-mass radius of $r_h = 7.24^{+1.94}_{-1.29}$ pc obtained using a Plummer profile. We carefully estimate the object total luminosity by means of direct integration of the background decontaminated LF. With the aid of a statistical bootstrapping we estimate the uncertainties on the total absolute magnitude of Balbinot 1 leading to the final value of $M_V = -1.21 \pm 0.66$.

Table 1
Summary of the derived parameters for Balbinot 1.

Parameter	Value	Unity
α_{J2000}	$22:10:43.15 \pm 0.3$	h:m:s
δ_{J2000}	$14:56:58.8 \pm 2.0$	$\circ:':''$
$d_{\odot}$	$31.9^{+1.0}_{-1.6}$	kpc
M_V	-1.21 ± 0.66	mag
$log(age/yr)$	$10.07^{+0.05}_{-0.03}$	dex
$[Fe/H]$	$-1.58^{+0.08}_{-0.13}$	dex
Plummer		
r_s	$0.6^{+0.16}_{-0.11}$	arcmin
Σ_{bg}	$1.38^{+0.03}_{-0.05}$	stars/arcmin^2
M^*	94.7 ± 5.9	
r_h	$0.78^{+0.21}_{-0.14}$	arcmin
King		
r_c	$0.22^{+0.10}_{-0.06}$	arcmin
r_t	$7.85^{+4.15}_{-3.40}$	arcmin
Σ_{bg}	$1.32^{+0.09}_{-0.07}$	stars/arcmin^2
Σ_c	162.76 ± 5.0	stars/arcmin^2
r_h	$0.69^{+0.33}_{-0.25}$	arcmin

In Table 1 we present a summary of the parameter derived for Balbinot 1.

The total number of stars and absolute magnitude of Balbinot 1 suggest that it is a star cluster. Its size is larger than that of most clusters in the Galactic system, either open or globular, or in M31 (Schilbach et al. 2006; van den Bergh 2010, 2011). However, it falls close to the median radius when compared to outer halo clusters in the Galaxy. Its size is more typical of the diffuse star clusters found by Peng et al. (2006) in early-type galaxies, but again with several orders of magnitude difference in terms of luminosity. It is an extremely low luminosity cluster; In fact, Balbinot 1 seems to be one of the faintest and lowest surface brightness old stellar systems found so far in the MW. Only Munoz 1 has a lower surface brightness (Muñoz et al. 2012), and only Munoz 1 and Segue 3 have lower absolute magnitudes. Its location in the luminosity vs. size diagram places Balbinot 1 close to other systems identified as low luminosity outer halo clusters, including Koposov 1 and AM4 (Fadely et al. 2011).

The stellar cloud that lies closest to Balbinot 1 is the Hercules-Aquila (Belokurov et al. 2007). The cloud is located at $l \sim 50°$ although its extension is poorly known, specially in the southern galactic hemisphere. However the heliocentric distance of the cloud is $10-20$ kpc, making it unlikely that Balbinot 1 is associated with this halo structure.

The small size of the object, and the lack of any clear evidence for complex stellar populations make it unlikely that it is a dwarf galaxy (Willman & Strader 2012). We note that this locus is at the confluence of the branches filled by classical globular clusters and MW dwarfs, as shown for instance in McConnachie (2012). Spectra from individual stars are being obtained and will allow measurement of metallicity spread and line-of-sight velocities, which may help determine the dynamical mass of Balbinot 1 and constrain its stellar population.

[1] The scale transformation from sky to physical values is 9.28 pc/arcmin

REFERENCES

Aihara, H. et al. 2011, ApJS, 193, 29
Belokurov, V., Walker, M. G., Evans, N. W., et al. 2010, ApJ, 712, L103
Belokurov, V., Evans, N. W., Bell, E. F., et al. 2007, ApJ, 657, L89
Belokurov, V., Zucker, D. B., Evans, N. W., et al. 2006, ApJ, 642, L137
Bertin, E., & Arnouts, S. 1996, A&AS, 117, 393
Cardelli, J. A., Clayton, G. C., & Mathis, J. S. 1989, ApJ, 345, 245
Fadely, R., Willman, B., Geha, M., et al. 2011, AJ, 142, 88
Girardi, L., Bertelli, G., Bressan, A., et al. 2002, A&A, 391, 195
Irwin, M. J., Belokurov, V., Evans, N. W., et al. 2007, ApJ, 656, L13
Kerber, L. O., & Santiago, B. X. 2009, IAU Symposium, 256, 391
Koposov, S., Belokurov, V., Evans, N. W., et al. 2008, ApJ, 686, 279
Koposov, S., de Jong, J. T. A., Belokurov, V., et al. 2007, ApJ, 669, 337
Larsen, S. S., & Brodie, J. P. 2000, AJ, 120, 2938
Majewski, S. R., Skrutskie, M. F., Weinberg, M. D., & Ostheimer, J. C. 2003, ApJ, 599, 1082
McConnachie, A. W. 2012, AJ, 144, 4
Muñoz, R. R., Geha, M., Côté, P., et al. 2012, ApJ, 753, L15
Martin, N. F., de Jong, J. T. A., & Rix, H.-W. 2008, ApJ, 684, 1075
Newberg, H. J., Willett, B. A., Yanny, B., & Xu, Y. 2010, ApJ, 711, 32
Peng, E. W., Côté, P., Jordán, A., et al. 2006, ApJ, 639, 838

Rocha-Pinto, H. J., Majewski, S. R., Skrutskie, M. F., Crane, J. D., & Patterson, R. J. 2004, ApJ, 615, 732

Rockosi, C. M., Odenkirchen, M., Grebel, E. K., et al. 2002, AJ, 124, 349

Rossetto, B., Santiago, B., Girardi, L., Camargo, J., Balbinot, E., da Costa, L., et al. 2011, AJ, 141, 185

Schilbach, E., Kharchenko, N. V., Piskunov, A. E., Röser, S., & Scholz, R.-D. 2006, A&A, 456, 523

Schlegel, D. J., Finkbeiner, D. P., & Davis, M. 1998, ApJ, 500, 525

Stetson, P. B. 1994, PASP, 106, 250

Tollerud, E., Bullock, J., Strigari, L., & Willman, B. 2008, ApJ, 688, 277

van den Bergh, S. 2011, PASP, 123, 1044

van den Bergh, S. 2010, AJ, 140, 1043

Walsh, S. M., Willman, B., & Jerjen, H. 2009, AJ, 137, 450

Willman, B., & Strader, J. 2012, AJ, 144, 76

Willman, B., 2010, Advances in Astronomy, 2010

Willman, B., Blanton, M. R., West, A. A., et al. 2005, AJ, 129, 2692